RD20/CLO3, a stress-induced calcium-binding protein, acts as a negative regulator of GPA1 in Arabidopsis through GAP activity

Justin Wright

A Thesis
In
The Department
Of
Biology

Presented in Partial Fulfillment of the Requirements
For the Degree of Master of Science (Biology) at
Concordia University
Montreal, Quebec, Canada

January 2014

© Justin Wright, 2014

CONCORDIA UNIVERSITY

School of Graduate Studies

This is to certify that the thesis prepared

By: Justin Wright

Entitled: RD20/CLO3, a stress-induced calcium-binding protein, acts as a negative regulator of GPA1 in Arabidopsis through GAP activity

and submitted in partial fulfillment of the requirements for the degree of

Master of Science (Biology)

complies with the regulations of the University and meets the accepted standards with respect to

originality and quality.

Signed by the final Examining Committee:

Patrick Gulick_____ Chair

Luc Varin_____ Examiner

William Zerges_____ Examiner

Reginald Storms_____ External Examiner

Patrick Gulick_____ Supervisor

Approved by _____
Chair of Department or Graduate Program Director

_____ 2014

_____
Dean of Faculty

ABSTRACT

RD20/CLO3, a stress-induced calcium-binding protein, acts as a negative regulator of GPA1 in Arabidopsis through GAP activity

Justin Wright

G-protein and calcium signaling have both been shown to play a role in the response to environmental abiotic stress in plants; however, the interaction between calcium-binding proteins and G-protein signaling molecules remains elusive. This study examines the interactions between RD20/CLO3 and Gα (the alpha subunit of the G-protein complex) from Arabidopsis, and their closest homologs, Ta-CLO3 and Ta-GA3 in wheat (*Triticum aestivum)*. Using *in vitro* GTPase assays, it is demonstrated that RD20/CLO3 and Ta-CLO3 have GTPase-activating protein (GAP) activity toward GPA1 and Ta-GA3, respectively, and this activity is potentiated by high calcium levels indicative of stress conditions. Phenotypic examination of mutant plants reveals a pattern of phenotypes congruent with the hypothesis of RD20/CLO3 acting as a downregulator of GPA1 activity. These findings reveal a novel role for RD20/CLO3 in regulating plant stress response. Furthermore, this work sheds light on the molecular mechanisms involved in controlling stomatal density under abiotic stress. *In vivo* interactions were tested through bimolecular fluorescence complementation (BiFC) with other caleosin proteins to further characterize the caleosin gene family. The work contributes to the understanding of G-protein signaling in response to environmental stress conditions.

ACKNOWLEDGMENTS

Many thanks to my supervisor, Dr. Patrick Gulick, and my committee members, Dr. Luc Varin and Dr. Bill Zerges, as well as my other lab members, Zhejun Wang, Hala Khalil, Alex Ralevski, Mohammad-Reza Ehdaeivand, Rob Carson, Gajra Garg, and in particular Sabrina Brunetti.

Additional thanks to Chloe van Oostende and the Centre for Microscopy At Concordia (CMAC), to Dr. Daniel McLaughlin and Angela Rose Lapierre, to Dr. Chris Brett, Dr. Marc Champagne, Dr. Peter Ulycznyj, the Centre for Structural and Functional Genomics (CSFG), and Concordia University.

TABLE OF CONTENTS

LIST OF FIGURES

LIST OF TABLES

Table 1. Guide to gene and protein names commonly mentioned

Gene name	**Protein name**	**Notes**
RD20/CLO3	RD20/CLO3, RD20, or At-CLO3	In literature, referred to either as RD20 or CLO3; this study will always use RD20/CLO3; "CLO3" alone will refer to Ta-CLO3
GPA1	Gα or GPA1	
AGB1	Gβ or AGB1	
AGG1	Gγ or AGG1	
Ta-*CLO3*	Ta-CLO3	Closest homolog of *RD20/CLO3* in wheat
Ta-*GA3*	Ta-GA3, Gα	Closest homolog of *GPA1* in wheat

"Ta-" before a gene name indicates that the gene is from *Triticum aestivum*; "At-" before a gene name indicates *Arabidopsis thaliana*.

INTRODUCTION

1. INTRODUCTION TO STRESS RESPONSE

The adverse effects of abiotic stresses, such as drought, salt, and cold, on plants has long been a major obstacle in agriculture. With the advent of climate change and limited water supplies, increased desertification has gained particular attention as an imminent threat to agricultural yields. A 2007 estimate concluded that 10-20% of Earth's drylands have already been degraded by desertification (Holtz 2007). By 2025, if current trends continue, an estimated 1.8 billion people could live in regions affected by water scarcity, and water stress could affect two thirds of the world population (World Bank 2009). The development of new varieties of crops tolerant to drought and other abiotic stresses is crucial, but is limited by our current understanding of the genetic and physiological stress-response mechanisms already existing in plants. Breeding techniques in cereal crops have traditionally selected for broad phenotypes rather than specific genes, but progress in this approach has been constrained by overlapping stress-response mechanisms and the overall complexity of the plant's stress-response network (Fleury 2010). Uncovering the genetic basis for the control of plant stress responses will allow for breeding techniques that select for specific loci rather than overall phenotypes, as well as reveal candidate genes for biotechnology-oriented approaches.

Plant physiological responses to abiotic stresses include osmotic changes to decrease water loss and increase water uptake (Chen and Jiang 2010), alterations in root architecture (Xiong *et al.* 2006), and changes in flowering time (Yaish *et al.* 2011). Modifications in root development in response to water stress include suppression of lateral root formation and stimulation of primary root penetration deeper into the soil where water concentration

tends to be higher (Xiong *et al.* 2006). On a molecular level, these responses are controlled by a vast set of interconnected pathways. When a plant is exposed to either abiotic or biotic stresses, early general responses include rapid compartment-specific changes in Ca^{2+} and reactive oxygen species (ROS) concentrations that follow patterns specific to certain stimuli (Wurzinger *et al.* 2011). Calcium-dependent pathways are triggered by the change in Ca^{2+} concentration, and include calcium-dependent protein kinases (CDPKs) and calcineurin B-like proteins (CBLs), all of which detect Ca^{2+} through EF-hand domains and activate downstream targets (Luan 2009). Mitogen-activated protein kinases (MAPKs) respond to external stimuli and activate phosphorylation cascades, eventually transducing the stimuli into transcriptional regulation (Wurzinger *et al.* 2010). Many of these mechanisms are interconnected with the production of the plant hormone abscisic acid (ABA), which is produced at high levels under abiotic stress conditions, as well as certain biotic stimuli, and serves as a transcriptional regulator for a number of stress-response proteins.

2. THE CALEOSIN GENE FAMILY

Triticum aestivum, commonly known as bread wheat, is recognized as the most robust major crop in the face of abiotic stresses (Tardif *et al.* 2007), and is capable of surviving temperatures as low as -21°C following an acclimation period. In the search for stress signalling genes, microarray analyses comparing cold-tolerant winter wheat to cold-sensitive spring wheat revealed a number of genes that were both more highly-expressed and more highly-induced during cold acclimation in cold-tolerant varieties than in cold-sensitive varieties (Gulick *et al.* 2005; Monroy *et al.* 2007). Among the most highly-induced genes in cold-tolerant wheat was Ta-*CLO3*, formerly named *J900,* which was induced 9-fold in cold-tolerant wheat following cold acclimation (Gulick *et al.* 2005; Monroy *et al.* 2007). (A guide to gene and protein names used in this study can be found in **Table 1**). Subsequent yeast-two-hybrid screening revealed interaction between Ta-CLO3 and a protein highly similar

in sequence to the alpha subunit, Ta-GA1, of the heterotrimeric G-protein complex (Tardif *et al*. 2007), described in section 4, suggesting possible involvement of the Gα protein in cold acclimation.

A homolog of *CLO3* in Arabidopsis, *RD20/CLO3* (At2G33380), which is a member of the caleosin gene family of calcium-binding genes, is strongly-induced under a variety of abiotic stress conditions, including dehydration, salt, cold, and ABA treatment (Takahashi *et al*. 2000). *RD20/CLO3* has also been identified as a regulator of stomatal control, and *rd20/clo3* mutants have exhibited decreased tolerance to drought and salt conditions (Aubert *et al*. 2010). *RD20/CLO3* is suggested to act as a stress signalling hub that triggers or regulates a plant's stress response mechanisms (Aubert *et al*. 2010).

The caleosin gene family is a small family of proteins that bind calcium through a single EF-hand domain. In Arabidopsis, 7 proteins have been identified as caleosins, but *RD20/CLO3* is the only member shown to be highly induced by abiotic stress conditions (Aubert *et al.* 2010). Recent evidence suggests that Arabidopsis *CLO4* is a negative regulator of ABA-mediated stress response, showing an expression pattern opposite to that of *RD20/CLO3* (Kim *et al*. 2011). Mutants lacking *CLO4* showed enhanced drought tolerance, while mutants lacking *RD20/CLO3* were more drought-sensitive (Kim *et al*. 2011, Aubert *et al*. 2010). Because *RD20/CLO3* is the only caleosin shown to exhibit stress induction, there has been little research reported on the remaining members.

Arabidopsis caleosin *CLO7* is the furthest in sequence similarity to wheat Ta-*CLO3*, while *CLO2* is highly similar to *RD20/CLO3* - these genes therefore serve as indicators of the conservation and variability of function in the caleosin family.

3. STRESS SIGNALING THROUGH CALCIUM

The binding of *RD20/CLO3* to calcium through an EF-hand domain suggests involvement in Ca^{2+}-mediated signalling pathways. Ca^{2+} concentration is normally main-

tained at low levels in the cytoplasm, and very high levels in the vacuole and endoplasmic reticulum, through active transport. Stress conditions, either through abscisic acid (ABA) signalling or through other signalling pathways, trigger ion channels to allow the passive flow of Ca^{2+} back into the cytoplasm (Sanders *et al*. 2002). The influx of Ca^{2+} into the cytosol occurs in patterns specific to the stressor – stomatal aperture, for example, is determined by the frequency and amplitude of $[Ca^{2+}]^{cyt}$ oscillations (Allen *et al*. 2001), while certain biotic stresses can result in a sustained increase in $[Ca^{2+}]^{cyt}$ levels (Lecourieux *et al*. 2005).

The signals encoded in the release of Ca^{2+} into the cytosol are then decoded by calcium sensor proteins. These sensors can be divided into either sensor responders, which detect calcium and directly play an activating role in response (such as phosphorylation), or sensor relays, which act through interaction with other proteins (Sanders *et al*. 2002). Calcium-dependent protein kinases (CDPKs) are sensor responder proteins that cause a phosphorylation cascade in response to calcium. Arabidopsis Calcium-dependent Protein Kinase3 (CPK3) and CPK6, for example, play a role in stomatal closure (Mori *et al*. 2006). Calcineurin B-like (CBL) proteins act as sensor relays, acting on CBL-Interacting Protein Kinases (CIPKs), and function as a broad signalling network, with great precision in detecting $[Ca^{2+}]$ gradients within the cytoplasm (Dodd *et al*. 2010).

4. THE PLANT HETEROTRIMERIC G-PROTEIN COMPLEX

The plant heterotrimeric GTP-binding protein (G protein) complex has been shown to play a role in the response to a number of stress conditions including high salinity, drought (Misra *et al*. 2007), light (Lapik and Kaufman 2003), hypoxia, and ethylene (Steffens and Sauter 2010), as well as biotic stress (Aharon *et al*. 1998). Components of the heterotrimeric G-protein complex have also been shown to act in signaling pathways regulated by abscisic acid (ABA) (Ritchie and Gilroy 2000; Wang *et al*. 2001; Pandey *et al*. 2006), jasmonic acid (Okamoto *et al*. 2009), and gibberellin (Ullah *et al*. 2003). G proteins and G-protein regula-

tors have been shown to be involved in alterations in root growth (Chen *et al.* 2006) and transpiration efficiency (Nilson and Assmann 2010); however, their integration into the stress signalling networks is still not well-understood.

The structure and role of the G-protein complex has been studied extensively in mammals, but remains a relatively new and unknown area of study in plants. In contrast to the mammalian G-protein complex, in which entire gene families exist for each subunit, plants contain very few genes coding for G proteins – the Arabidopsis genome, for example, has only one gene each encoding Gα and the Gβ subunits, two genes encoding Gγ-subunits (Jones and Assmann, 2004) one gene encoding a Regulator of G-protein-signaling (RGS1) protein, and one known G-protein-coupled receptor (GPCR) (Urano and Jones 2013). The low number of genes encoding heterotrimeric G proteins in plants suggests that diversity of signalling through the G-protein signalling pathways may derive from diversity of proteins that interact with them, but this hypothesis is just begining to be examined. Mechanisms for regulating G-protein signalling through interactions with Gα include GTPase-activating proteins (GAPs), which increase Gα's rate of GTP hydrolysis, favouring the return to its inactive state, and guanine-nucleotide exchange factors (GEFs), which have the opposite effect.

Both *RD20/CLO3* and *GPA1,* the Arabidopsis gene encoding the *α*-subunit of the heterotrimeric G protein, have been shown to be regulators of transpirational efficiency (TE) in Arabidopsis (Aubert *et al.* 2010; Nilson and Assmann 2010). TE is the ratio of plant growth to water loss via transpiration, and is used as an indicator of the effectiveness of a plant's use of water (Nilson and Assmann 2010). Nilson and Assmann (2010) showed that enhanced transpirational efficiency of *gpa1* mutants was likely due to reduced stomatal density (resulting in fewer outlets for water loss), and not to altered response of stomata opening or closing to drought. The *RD20/CLO3* overexpressor was also shown to have increased transpirational efficiency, while the *rd20/clo3* mutant exhibited the opposite characteristic; the physiological basis of altered efficiency was not investigated.

Gα, Gβ, and RGS1 have been identified as regulators of root morphology (Chen *et al.* 2006). Pandey *et al.* (2006) found that *gpa1* mutant plants responded to exogenous exposure to ABA with a higher reduction in primary root elongation than wild type plants. Mutants of *AGB1,* the gene coding for Gβ, showed an increase in lateral root production, while *gpa1* mutants showed a decrease in lateral roots. Triple mutants lacking *RGS1* (coding for RGS, regulator of G-protein signalling), *GPA1,* and *AGB1* showed an even higher increase in lateral root number than *agb1* mutants, as well as an increase in root meristematic cell division, suggesting that the G-protein complex containing an inactive Gα subunit normally suppresses lateral root formation (Chen *et al.* 2006). In examining the effect of glucose on root architecture, Booker *et al.* (2010) found that null mutations in either *GPA1* or *RGS1* fully cancelled out the effect of glucose, which normally stimulates lateral root production, but double mutants of *GPA1* and *AGB1* or single mutants of *AGB1* did so only partially. They therefore proposed that Gα stimulates lateral root emergence by inhibiting Gβ, and possibly through an additional direct pathway (Booker *et al.* 2010). If RD20/CLO3 inhibits Gα activity in root tissue, it could potentially play a role as an inhibitor of lateral root emergence and a promoter of primary root elongation.

To date, few upstream G-protein-coupled receptors have been shown to interact with the Gα subunit of Arabidopsis, namely AtGCR1 (Pandey and Assmann, 2004), regulator of G protein signaling protein 1 (AtRGS1) (Chen *et al.* 2003), and GPCR-type G-protein (GTG) 1 and GTG2 (Pandey *et al* 2009). Similarly, few presumably downstream interactors have been identified that physically interact with the plant Gα subunit. The Gα subunit of Arabidopsis, GPA1, interacts with the Arabidopsis cupin domain protein ATPIRIN1 which regulates seed germination and seedling development (Lapik and Kaufman 2003). Phospholipase D (PLDα1) (Zhao and Wang 2004), prephenate dehydratase protein (PD1) (Warpeha *et al.* 2006); the plastid protein thylakoid formation 1 (THF1) of Arabidopsis were shown to interact with GPA1 in Arabidopsis (Huang *et al.* 2006) and in *Eschscholzia californica,* phospholipase A_2 (PLA_2) was found to interact with Gα (Heinze *et al.* 2007).

5. PROJECT GOAL

The present project aims to investigate the mechanism and role of the interaction between *GPA1* and *RD20/CLO3,* and their wheat homologs *Ta-GA3* and *Ta-CLO3.* Existing knowledge suggests the potential role of the RD20/CLO3 protein as a negative regulator of GPA1. This hypothesis is examined at the molecular level *in vitro* and at a phenotypic level. Additional interactions between other members of the caleosin gene family and components of the G-protein complex are examined *in vivo* to further understand the caleosin gene family as a whole.

MATERIALS AND METHODS

Plant growth conditions

Soil-grown plants

For the growth of the wild tobacco, *Nicotiana benthamiana,* a soil mixture containing equal parts of black earth, peat moss, and vermiculite were mixed and heated at 150°C for one hour. Dry seeds were stratified in the dark at 4°C for 2-3 days prior to sowing. Tobacco seedlings were grown in a growth chamber at, 43.21 $\mu mol \cdot m^{-2} \cdot s^{-1}$ fluorescent light with a light cycle of 16 hr light and 8 hr dark unless otherwise stated.

Arabidopsis plants were grown in the soil mixture described above. Seeds were sown in soil and stratified in the dark at 4°C for 3-4 days. Pots were then placed in growth chambers and grown under the same conditions as the *N. benthamiana* plants.

Plants grown on agar based media

Growth of Arabidopsis plants was also characterized on agar media plates. Seeds were sterilized by vortexing in 70% ethanol followed by a sterilization solution (30% bleach, 1% Triton X-100) for 7 min, washed 4-5 times with distilled water, and stratified in the dark at 4°C for 3-4 days. Seeds were plated on petri dishes containing sterile media consisting of 0.5x Murashige and Skoog basal salt mixture, 1% (w/v) Sucrose, 0.05% MES hydrate (4-Morpholineethanessulfonic acid), 0.4% Gelzan™ CM agar substitute gelling agent adjusted to pH 5.7. To measure root growth in response to hormone treatment, plants were grown on MS plates for 48 hours and then transferred to abscisic acid treatment plates (MS media, 1% sucrose, and 2 μM ABA), or control plates (only MS media and 1% sucrose) and grown for 8 days with the plates positioned near vertically. To prevent contact between leaf tissue and sucrose in the MS media, which may alter lateral root formation, the top section of media of each plate was removed as suggested by (Dubrovsky and Forde 2012).

Sources of seeds

Seeds for transgenic Arabidopsis with the GPA1 promoter:*GUS* fusion, as well as seeds containing a mutation in *GPA1* (*gpa1-2* mutants) were kindly provided by Sarah Assmann (Pennsylvania State U.). All other seeds were purchased from the Arabidopsis Biological Resource Center (ABRC).

Generation of expression vectors

DNA sources

Arabidopsis genomic DNA was purified using the REDExtract-N-Amp™ Plant PCR Kit (Sigma) with a protocol similar to the manufacturer's instructions. Tissue samples of approximately 0.5 cm^2 were cut from leaves of mature Arabidopsis plants of the Colombia (Col-0) ecotype using a razor blade. 50 µL Extraction Solution and 50 µL Dilution Solution were used, and DNA was stored at -20°C.

All Arabidopsis cDNA clones were ordered either from the Arabidopsis Biological Resource Center (ABRC) at the Ohio State University, the RIKEN BioResource Center in Japan, or were obtained from Dr. Alan Jones. Sources of cDNA for each clone are shown in **Table 2**.

Generation of entry clones and expression vectors

The coding regions from cDNA clones were amplified by PCR using primers with Gateway® recombination sites and cloned into pDonr201 or pDonr207 by Gateway® in vitro recombination using the BR Clonase II Enzyme mix (Invitrogen). Constructs were transformed into the TOP10 *E. coli* strain by electroporation, and plasmid was purified from the *E. coli* culture. Gateway® LR reactions were used to transfer the inserts from entry vectors to binary destination vectors including the bimolecular fluorescence complementation vectors (BiFC) pBatTL-B-sYFP-C, and pBatTL-B-sYFP-N, to create C-terminal half Yellow Fluorescent Protein (YFP), and N-terminal half-YFP fusions respectively. Coding sequenc-

Table 2. *Entry clones used in this study*

Construct	Gene name	Vector description	cDNA source
Gβ-pDONR201	*AGB1**	Entry clone	Alan Jones
Gγ-pDONR201	*AGG1**	Entry clone	Alan Jones
CLO1-pDONR201	*CLO1**	Entry clone	RIKEN-BRC[a]
CLO2-pDONR201	*CLO2**	Entry clone	ABRC[b]
CLO7-v1-pDONR201	*CLO7-v1**	Entry clone	INRA[c]
1st half RD20/CLO3-pDONR201	*RD20CLO3 (1st half)*	Truncated (1st half) of sequence	ABRC[b]
2nd half RD20/CLO3-pDONR201	*RD20/CLO3 (2nd half)**	Truncated (2nd half) of sequence	ABRC[b]
ERECTA-pDONR201	*ERECTA**	Entry clone	RIKEN-BRC[a]
PLC1-pDONR201	*Pi-PLC1**	Entry clone	ABRC[b]
PLC7-pDONR201	*Pi-PLC7**	Entry clone	ABRC[b]

* indicates no stop codon
a RIKEN BioResource Center (RIKEN BRC), Japan
b Arabidopsis Biological Resource Center (ABRC), Ames, USA
c Institute National de la Recherché Agronomique (INRA), France

Table 3. *Expression vectors used in this study*

Construct	Gene name	Vector description	Source
Gα-pBatTL-B-sYFP-C	*GPA1**	Fusion with C-terminal subunit of YFP	Zhejun Wang
Gβ-PK7FWG2	*AGB1**	eGFP fusion	Justin Wright
Gβ-pBatTL-B-sYFP-C	*AGB1**	Fusion with C-terminal subunit of YFP	Justin Wright
Gβ-pBatTL-B-sYFP-N	*AGB1**	Fusion with N-terminal subunit of YFP	Justin Wright
Gγ-PK7FWG2	*AGG1**	eGFP fusion	Justin Wright
Gγ-pBatTL-B-sYFP-C	*AGG1**	Fusion with C-terminal subunit of YFP	Justin Wright
Gγ-pBatTL-B-sYFP-N	*AGG1**	Fusion with N-terminal subunit of YFP	Justin Wright
CLO7-v1-PK7FWG2	*CLO7-v1**	eGFP fusion	Justin Wright
CLO7-v1-pBatTL-B-sYFP-C	*CLO7-v1**	Fusion with C-terminal subunit of YFP	Justin Wright
CLO7-v1-pBatTL-B-sYFP-N	*CLO7-v1**	Fusion with N-terminal subunit of YFP	Justin Wright
CLO7-v3-pBatTL-B-sYFP-N	*CLO7-v3**	Fusion with N-terminal subunit of YFP	Zhejun Wang
CLO2-PK7FWG2	*CLO2**	eGFP fusion	Justin Wright
CLO2-pBatTL-B-sYFP-C	*CLO2**	Fusion with C-terminal subunit of YFP	Justin Wright
CLO2-pBatTL-B-sYFP-N	*CLO2**	Fusion with N-terminal subunit of YFP	Justin Wright
RD20/CLO3-pFAST-G02	*RD20/CLO3**	35s promoter for overexpression	Justin Wright
RD20/CLO3-pDEST17	*RD20/CLO3**	RD20/CLO3 with 6xHis tag	Zhejun Wang
GPA1-pDEST17	*GPA1**	GPA1 with 6xHis tag	Alan Jones
Ta-CLO3-pDEST17	*RD20/CLO3**	Ta-CLO3 with 6xHis tag	Hala Khalil
Ta-GA3-pDEST15	*Ta-GA3**	Ta-GA3 with GST tag	Hala Khalil

*indicates that no stop codon was included in the clone

es were also subcloned by Gateway® LR reactions as fusions to full length enhanced Green Fluorescent Protein (eGFP), in the PK7FWG2 binary vector. For protein expression in *E. coli*, coding sequences were transferred from entry clones to pDEST17, with a Gateway®-compatible 6-His-tag N-terminal fusion (Invitrogen). The expression vector for His-tagged *GPA1* was a gift from Dr. Alan Jones (North Carolina State University). A list of entry clones generated and used is found in **Table 2**.

To localize *RD20/CLO3* expression in Arabidopsis by GUS reporter expression, the region 1000 bp before the transcription start site, more than enough to contain the entire promoter region, was amplified by PCR, and cloned into the binary vector pKGWFS7. The *promoterGPA1:GUS* construct was obtained from Sarah Assmann (Pennsylvania State U.), and contained the region 1500 bp before the transcription start site in the binary GUS vector pORE R1.All constructs were verified by PCR, and entry clones were verified by PCR and sequencing. When it was found that the constructs of both *CLO7-v1* and *AGG1* contained errors, the genes were re-cloned and the experiment repeated. The new clones produced the positive interactions described in the results.

Gene expression in plants

Transformation of Agrobacterium tumefaciens

Expression vectors were transformed into *Agrobacterium tumefaciens* for later transformation into plants. *Agrobacterium* strain AGL1 was used originally, but was later replaced by LBA4404 for improved transformation efficiency. Cells were transformed by electroporation, and grown on plates with LB media for two days at 30°C.

Expression profiling through β-glucuronidase (GUS) reporter assay

Transgenic plants containing *promoterRD20/CLO3:GUS* seed were germinated on control MS media with 1% sucrose. After three, five, six, or ten days, plants were transferred to MS plates with 1% sucrose supplemented with either 10 μM ABA or to control media. The plants were treated for 6 hours, and then transferred to an X-Gluc solution made ac-

cording to the protocol described in Jefferson *et al.* (1987). Samples were then destained in 70% ethanol after staining for 24 hours.

Plants expressing *promoterRD20/CLO3:GUS* were also grown in soil for 13 days after germination in soil, then were sprayed twice per week with either ABA solution (25 μM ABA, .5% ethanol), or control solution (.5% ethanol). These plants were then stained for 24 hours in the X-Gluc solution described previously.

Tissue embedding and sample sectioning

To examine cell-specific gene expression by GUS reporter assay, leaf tissue samples were embedded in paraffin using the "simplified paraffin embedding method" presented in Xing et al. (2009). Because the tissue samples were already submerged in 70% ethanol to destain the GUS assay, the first step of the protocol (placing the tissues in a fixative) was skipped. Embedded samples were sliced with a microtome into 3-micron-thick samples. To mount the samples on slides, the tissue-containing paraffin slices were placed on top of warm water; glass slides with a layer of egg white brushed onto the surface were used to pick up the slices from the surface of the water. After the slides dried, cover slips were placed over the slides with several drops of resin.

Bimolecular fluorescence complementation (BiFC) and GFP localization

Interactions were detected *in vivo* by BiFC, in which two genes were fused to the different halves of YFP, for expression in plant cells as described earlier in "*Generation of entry clones and expression vectors*". Fusions to full length eGFP also showed localization of individual proteins. To verify the subcellular localization of protein expression and interaction, specific organelle markers were co-expressed with the YFP or GFP fusions. These markers are shown in **Table 4**. Several of the markers proved to be problematic; the PM marker especially, in certain cells, showed expression in other organelles. This problem was partially rectified by infiltrating with a lower OD_{600}, but for many samples, the marker had to be left out entirely.

***Table 4**. Organelle markers as mCherry fusions*

Organelle	Construct name	Targeting Protein
PM	PM-rk CD3-1007	Full length of AtPIP2A, a plasma membrane aquaporin
Tonoplast	T-rk CD3-975	C-terminus of c-TIP, an aquaporin of the vacuolar membrane fused to the fluorescent protein
ER	ER-rk CD3-959	Signal peptide of AtWAK2, wall-associated kinase2, at N-terminus of protein and an ER retention signal, His-Asp-Glu-Leu, at the C- terminus.
Plastid	Pt- rk CD3-999	First 79 aa of small subunit of tobacco rubisco.
Mitochondria	Mt-rk CD3-991	First 29 aa of yeast cytochrome C oxidease IV.
Golgi	G-rk CD3-967	First 49 aa of GmMan1, soybean α-1,2 mannosidae 1.
Peroxisome	Px-rk CD3-983	Peroxisomal targeting signal1, Ser-Lys-Leu, at C- terminus of the fluorescent protein.

PM, Plasma Membrane; **T,** Tonoplast; **ER**, Endoplasmic Reticulum; **Pt**, Plastids; **Mt**, Mitochondria; **G**, Golgi; **PX**, Peroxisome; **r**, mCherry fluorescent protein; **k**, kanamycin resistance.

Plasmid constructs for use in bimolecular fluorescence complementation (BiFC) or localization for expression of protein fusions with full length green fluorescent protein (GFP) constructs and subcellular markers, were transformed into *Agrobacterium tumefaciens* strain LBA4404 and infiltrated into *N. benthamiana* leaves according to Kapila et al. (1997) with the minor modification that *Agrobacterium* infiltration solutions were used at both high and low cell concentrations, OD_{600} of 0.5 and 0.1. Three days after infiltration, 0.5 cm^2 sections were cut out from leaves and examined by microscope.

Microscopy

Leaf samples examined for BiFC and fluorescence localization were viewed and photographed with a confocal LSM Leica TCS SP2, controlled by the LeicaConfocal Software. The PL APO 40x oil objective (N.A: 1.25) was used, with a final image resolution of 1024 x 1024 pixels. For mCherry markers, a Helium-Neon laser (excitation wavelength of 543 nm; emission at 560-640 nm) was used at 100% intensity. For YFP interactions, an Argon laser (excitation wavelength of 514 nm; emission at 520-590nm) was used at 90% intensity. Additional samples were examined with a Zeiss Axioplan fluorescence microscope mounted with a Lumenera Infinity 3-1C 1.4 megapixel colour-cooled CCD camera using the 40x objective lens. The filters used were: GFP Filter Cube #1031346 (Exciter Filter: BP 470/40, Beam Splitter: FT 495, Barrier Filter: BP 525/30), dsRed Filter Cube #1114462 (Exciter

Filter: BP 560/40, Beam Splitter: FT 585, Barrier Filter: BP 630/75), and YFP Filter Cube #1196681 (Exciter Filter: BP 500/20, Beam Splitter: FT 515, Barrier Filter: BP 535/30). Tissue samples from plants expressing *RD20/CLO3* promoter:*GUS* constructs were examined under the Zeiss Axioplan fluorescence microscope, using the 10x objective lens in bright-field and dark field format.

GTPase assay

Protein purification from E. coli

His-tagged GPA1 was expressed in *E. coli* strain BL21 and purified using a modified version of the protocol described in Willard and Siderovski (2004). Cells were precultured overnight in 50 ml LB with 50 μM ampicillin, shaking at 37°C, and then transferred to 450 ml LB. The culture was shaken at 37°C until an OD_{600} of 0.6-0.9 was reached. The cells were induced with .5 mM IPTG overnight and then pelleted by centrifugation at 4°C for 45 minutes at 9500 rpm. The pellet was resuspended in 50 ml lysis buffer (50 mM Tris–HCl, pH 7.5; 100 mM NaCl; 5% (v/v) glycerol; 10 mM imidazole; 50 μM GDP; 5 mM $MgCl_2$; 30 μM $AlCl_3$; 20 mM NaF); lysozyme was added at 1 mg/ml and $MgCl_2$ was added to a final concentration of 20 mM, and the suspension was rocked for 30 minutes at 4°C. $AlCl_3$ and NaF were included because their reaction produces AlF_4, a molecule shown to increase the yield of Gα purification. The cell suspension was sonicated for 2 min. NaCl was added to bring the concentration to 300 mM, and the solution was rocked for 30 minutes at 4°C. The solution was centrifuged at 11000 x g for 35 min and the supernatant removed and incubated with rocking 90 min. lycerol, 5 mM $MgCl_2$, 30 μM $AlCl_3$, 20 mM NaF, 5 mM PMSF, 50 μM GDP, 1 mM DTT, and 3x Complete EDTA-free protease inhibitor (Roche) at 3 tablets/L). Recombinant Ta-GA3-GST protein was purified from the supernatant with Glutathione Sepharose™ 4B beads (GE Healthcare Life Sciences) according to the manufacturer's protocol by incubation for 90 min at 4°C with rocking. The matrix was rinsed twice in a chromatography column (Bio-Rad) with 137 mM NaCl, 2.7 mM KCl, 8.1 mM Na_2HPO_4, and 1.76 mM KH_2PO_4 and eluted with 25 mM glutathione, 50 mM Tris–HCl, pH 8.0, and 150 mM

NaCl. Purified GPA1-His is shown in **Figure 4**.

Ta-CLO3-His and RD20/CLO3-His were isolated from a bacterial pellet from a 1 L culture by suspension in 10 ml of B-PER lysis buffer (Pierce) and centrifuged at 11000 x g for 30 min. RD20/CLO3 protein was purified from the supernatant using Ni–NTA Agarose (Qiagen) according to Pandey et al. (2009) and stored in aliquots of 100 µl at -80°C.

Preparation of protein samples and detection of GTPase activity

Purified proteins were incubated with 2 mM EDTA for five min, and GTP was added to 5 mM final concentration and incubated for 30 min at 4°C. All protein samples were buffer-exchanged three times in 50 mM Tris–HCl, pH 7.5, and 100 mM NaCl at 4°C, with VivaSpin 500 columns (Stedim) according to the manufacturer's protocol. The GTPase reactions using wheat proteins were performed in the exchange buffer with 10 µM GTP and 10 mM $CaCl_2$. Proteins were assayed at approximately 50 µM each. The reactions were activated with 10 mM MgCl2 and incubated for 30 min at room temperature. Inorganic phosphate, the GTPase reaction product, was assayed using the P_iPer Phosphate assay kit (Invitrogen) according to the manufacturer's protocol, with samples being read over a 1 h time course. Results show the average of 3 assays.

Stomate density and leaf phenotypes

To characterize stomate density, leaf number, and the leaf length:width ratio in mutant *rd20/clo3* and *gpa1* plants and in controls, plants were grown in soil for 6 weeks during which time they were sprayed twice per week with a solution of 25 µM ABA and 0.05% ethanol. Control plants were sprayed twice per week with 0.05% ethanol (Nilson and Assmann 2010). Six plants were characterized for each genotype. Stomate density was measured microscopically for three leaves per plant using epidermal peels made from each leaf and photographed at 400x magnification with a Zeiss Axioplan fluorescence microscope with a Lumenera Infinity 3-1C 1.4 megapixel color-cooled CCD camera. Between nine and twelve photographs were examined per plant. To count the leaf number, leaves larger than

1 cm^2 were counted in each plant 6 weeks after germination. Leaf shape was measured by photos taken from above and analysed in Adobe® Photoshop®.

Statistical analysis

For protein assays and phenotype data, standard error was calculated for each group. A student's T-test was performed to detect statistical significance using a P of < 0.05.

Table 5. *Accession numbers for genes mentioned*

Arabidopsis		
Gene name	**TAIR accession**	**GenBank accession**
CLO1	AT4G26740.1	NM_118808.4
CLO2	AT5G29560.1	N/A
RD20/CLO3	AT2G33380.1	NM_128898.3
CLO4	AT1G70670.1	NM_105735.2
CLO7-v1	AT1G23240.1	N/A
CLO7-v3	AT1G23240.3	BX814132
PLC1	AT5G58670.1	NM_125254.1
PLC7	AT3G55940.1	NM_115452.1
AGB1	AT4G34460.1	NM_119611.4
AGG1	AT3G63420.1	NM_116207.2
GPA1	AT2G26300.1	NM_128187.3

Triticum aestivum	
Gene name	**GenBank accession**
Ta-GA3	HQ020506.1
Ta-CLO3	HQ020505.1

Table 6. *Primers used in this study*

Gene	Accession No.	Primer name	Direction	Sequence	T_m	Region	Product size	Stop?
CLO1	AT4G26740.1	CLO1F	Forward	***GGGGACAAGTTTGTACAAAAAAGCAGGCTTA***ATGGGGTCAAAGACGGAGAT	60	CDS	796 bp	No
		CLO1R	Reverse	***GGGGACCACTTTGTACAAGAAAGCTGGGTC***GTAGTATGCTGTCTTGTCTTCACTGAT	60			
ERECTA	AT2G26330.1	ERECTAF	Forward	***GGGGACAAGTTTGTACAAAAAAGCAGGCTTA***ATGGCTCTGTTTAGAGATATTGTTCTT	60	CDS	2989 bp	No
		ERECTAR	Reverse	***GGGGACCACTTTGTACAAGAAAGCTGGGTC***CTCACTGTTCTGAGAAATAACTTGTCC	60			
PLC1	AT5G58670.1	PLC1F	Forward	***GGGGACAAGTTTGTACAAAAAAGCAGGCTTA***ATGAAAGAATCATTCAAAGTGTGTTT	59	CDS	1744 bp	No
		PLC1R	Reverse	***GGGGACCACTTTGTACAAGAAAGCTGGGTC***ACGAGGCTCCAAGACAAACC	62			
PLC7	AT3G55940.1	PLC7F	Forward	***GGGGACAAGTTTGTACAAAAAAGCAGGCTTA***ATGTCGAAGCAAACATACAAAGTC	60	CDS	1813 bp	No
		PLC7R	Reverse	***GGGGACCACTTTGTACAAGAAAGCTGGGTC***CACAAACTCCAACCGCAC	59			
Gβ	AT4G34460.1	B1-Gβ	Forward	***GGGGACAAGTTTGTACAAAAAAGCAGGCTTA***ATGTCTGTCTCCGAGCTCAAA	60	CDS	1192 bp	No
		B2-Gβ3	Reverse	***GGGGACCACTTTGTACAAGAAAGCTGGGTC***AATCACTCTCCTGTGTCCTCC	58			
Gγ	AT3G63420.1	Gγ F2	Forward	***GGGGACAAGTTTGTACAAAAAAGCAGGCTTA***ATGCGAGAGGAAACTGTGGTT	61	CDS	358 bp	No
		Gγ R3	Reverse	***GGGGACCACTTTGTACAAGAAAGCTGGGTC***AAGTATTAAGCATCTGCAGCCTTC	60			
RD20/CLO3	AT2G33380.1	RD20GWFOR	Forward	***GGGGACAACTTTGTACAAAAAAGCAGGCTTC***ATGGCAGGAGAGGCAGAGGCTTT	67	CDS	772 bp	No
		RD20GWREV	Reverse	***GGGGACCACTTTGTACAAGAAAGCTGGGTA***GTCTTGTTTGCGAGAATTGGCCCT	67			

GPA1	AT2G26300.1	GPA1GWFOR	Forward	***GGGGACAACTTTGTACAAAAAAGCAGGCTTC***ATGGGCTTACTCTGCAGTAGAAGTCG	64	CDS	1213 bp	No
		GPA1GWREV	Reverse	***GGGGACCACTTTGTACAAGAAAGCTGGGTA***TAAAAGGCCAGCCTCCAGTAAATTTC	64			
TA-CLO3	HQ020505.1	J900GWFOR	Forward	***GGGGACAAGTTTGTACAAAAAAGCAGGCTTC***ATGGCGATCCGGCGACAAT	67	CDS	721 bp	No
		J900GWREV	Reverse	***GGGGACCACTTTGTACAAGAAAGCTGGGTC***CATTGCACTATGATGAGAAAAGGCCC	66			
CLO2	AT5G29560.1	CLO2F	Forward	***GGGGACAAGTTTGTACAAAAAAGCAGGCTYY***ATGACGTCGATGGAGAGGAT	47	CDS	721 bp	No
		CLO2R	Reverse	***GGGGACCACTTTGTACAAGAAAGCTGGGTY***GTAGTACGTCTTGTACTCCTTGATCTC	48			
CLO7-v1	AT1G23240.1	CLO7-v1F3	Forward	***GGGGACAAGTTTGTACAAAAAAGCAGGCTTC***ATGTCTCATCAGACAGTAGCGC	60	CDS	691 bp	No
		CLO7-v1R2	Reverse	***GGGGACCACTTTGTACAAGAAAGCTGGGTC***TGGTAGTTTTTGTTTCTTGCCA	60			

RESULTS

1. Protein-Protein interactions

CLO7-v1 interacts with Gα and Gγ

Interactions with various proteins in the caleosin family were examined to indicate the level of conservation within the gene family, and to provide a greater understanding of the gene family as a whole. CLO7 was tested because it was furthest in sequence similarity to wheat Ta-CLO3. CLO7 version 1, the most abundant splice variant of CLO7, showed positive interaction with GPA1 and AGG1. The interaction was localized primarily to the PM, and to a lesser extent in the tonoplast, as shown by co-localization with the PM marker (At-PIP2A) and tonoplast marker (C-terminus of γ–TIP, the aquaporin of the vacuolar membrane) (**Figure 1 and 2**). No interaction was seen in the ER, indicated by a lack of fluorescence observed in the ER network. An original clone of CLO7-v1 showed interaction only with AGG1, but not GPA1.

When CLO7-v1 was expressed as a fusion with eGFP, the protein was localized to the nucleus and what appears to be the plasma membrane (**Figure 1G-I**). AGG1 fused with eGFP appeared to be localized to the same organelles (**Figure 2G-I**). However, the low resolution of the microscope used, as well as improper localization of certain organelle markers, made it impossible to differentiate between the PM and other nearby organelles such as the tonoplast for both CLO7-v1 and Gγ. Fluorescence showed overlap with these organelles, but never in any regions that did not already overlap with the PM. Previous results from this lab that have yet to be published showed that GPA1, expressed as a fusion with eGFP, localizes primarily to the PM.

This unpublished data, from other lab members, also showed consistent interaction between GPA1 and RD20/CLO3 in BiFC assays. This interaction was used as a positive control for this study; the work is described in a manuscript that is in revision after review.

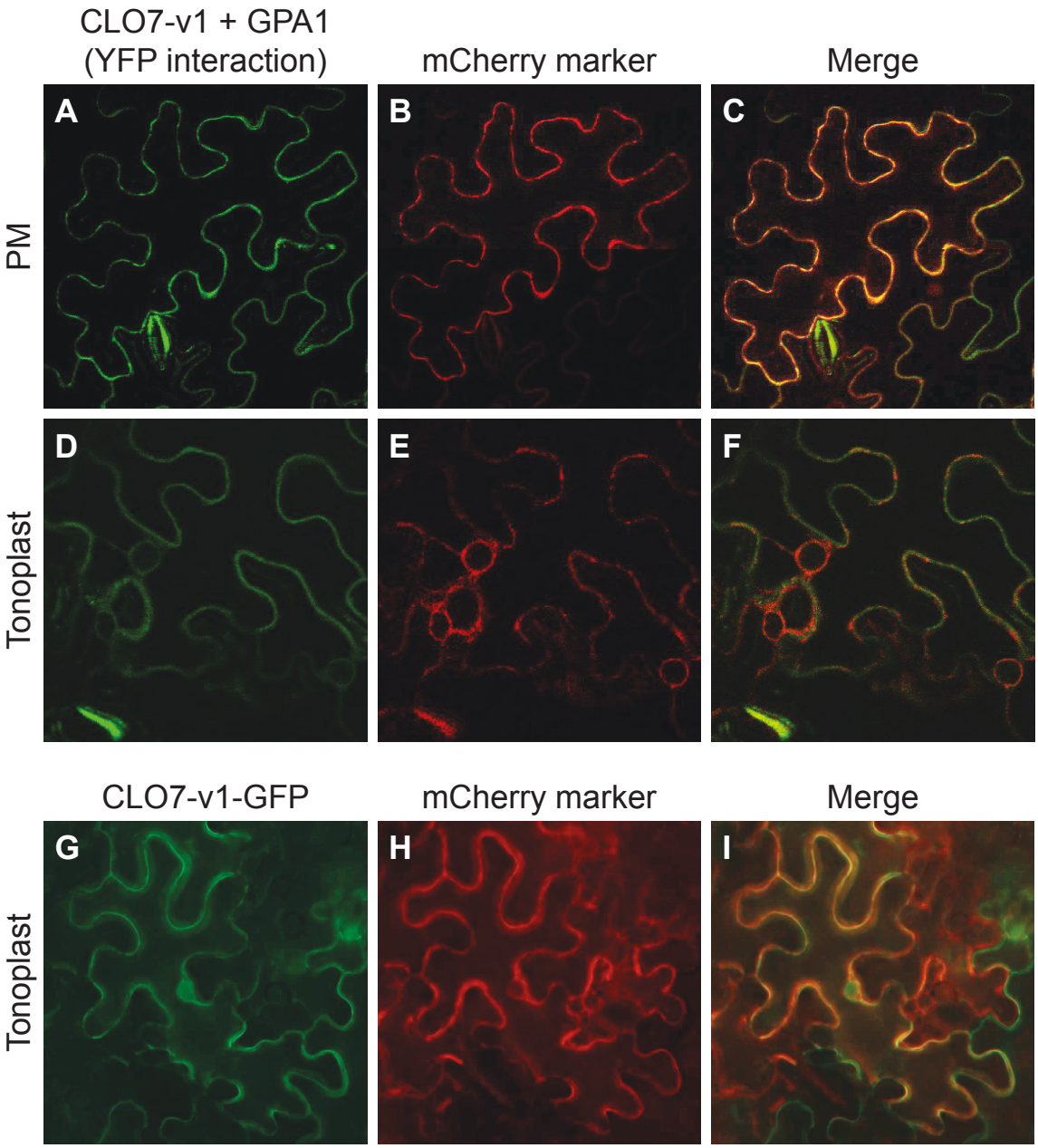

Figure 1. Interaction between CLO7-v1 and GPA1. **(A and D)** BiFC interaction of CLO7-v1- and GPA1-YFP fusions. **(B)** At-PIP2A-mCherry, a plasma membrane marker. **(E and H)** mCherry fusion with C-terminus of c-TIP, a tonoplast marker. **(C and F)** Merged images of interactions and markers. The interaction appears throughout the PM and overlaps significantly with the tonoplast marker. **(G)** Localization of CLO7-v1 fused to eGFP. **(I)** Merged images of CLO7-v1-GFP and tonoplast marker. Localization appears to be in the nucleus and PM, but the resolution of the microscope used is too low for accurate determination.

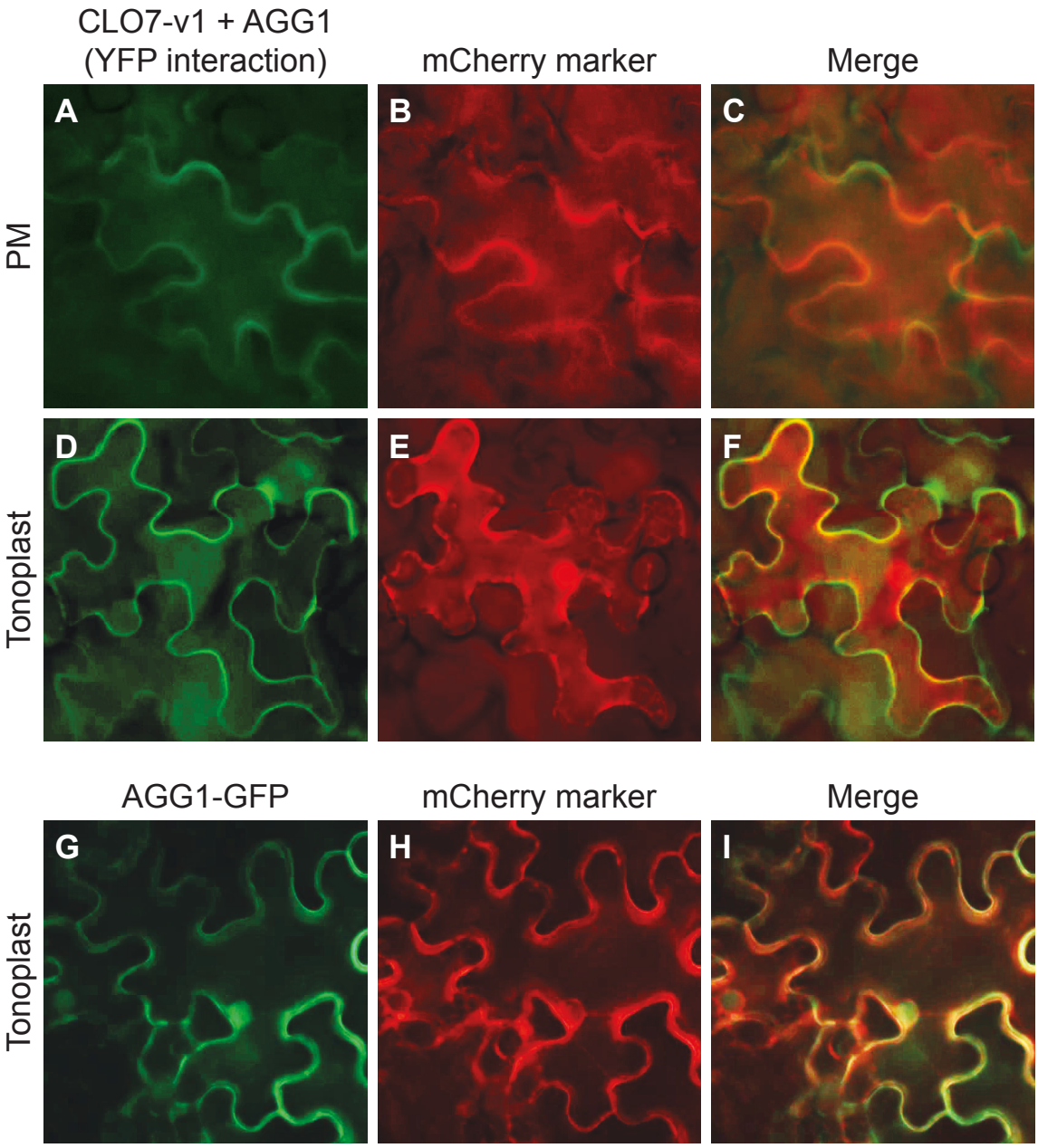

Figure 2. Interaction between CLO7-v1 and Gγ. **(A and D)** BiFC interaction of CLO7-v1- and Gγ-YFP fusions. **(B)** AtPIP2A-mCherry, a plasma membrane marker. **(E and H)** mCherry fusion with C-terminus of c-TIP, a tonoplast marker. **(C and F)** Merged images of interactions and markers. The interaction appears throughout the PM. The partial overlap with the tonoplast marker is inconclusive at this resolution. **(G)** Localization of fusion between Gγ and eGFP. **(I)** Merged images of AGG1-GFP and tonoplast marker. Like with CLO7-v1, localization appears to be in the nucleus and PM, but the resolution of the microscope used is too low for accurate determination.

Proteins showing no interaction

Of the interactions tested between G-protein subunits (specifically the α, β, and γ subunits) and members of the caleosin gene family (specifically CLO2, RD20/CLO3, CLO7-v1, and CLO7-v3), some did not show interaction - the exact pairs that did not interact are shown in **Table 7**. RD20/CLO3, which interacted with Gα, showed no interaction with the other subunits of the G-protein complex subunits, Gβ and Gγ. Neither splice variant of CLO7 showed interaction with AGB1. CLO2 was tested for interaction with GPA1, AGG1, AGB1, and RD20/CLO3, and no positive interactions were found. CLO7-v3, which had been previously shown to interact with GPA1, showed no interaction with Gγ, despite the fact that its splice variant, CLO7-v1, showed interaction with both. A summary of interaction data is shown in **Table 7**.

	CLO2	*RD20/CLO3*	*CLO7-v1*	*CLO7-v3*	*GPA1*	*AGB1*	*AGG1*
CLO2	-	-			-	-	-
RD20/CLO3	-	-	-	-	+	-	-
CLO7-v1		-	-		+	-	+
CLO7-v3		-		-	+	-	-
GPA1	-	+	+	+	-	+	+
AGB1	-	-	-	-	+	-	+
AGG1	-	+	+	-	-	+	-

Table 7. Summary of BiFC interaction data. Positive interactions are indicated by a plus, negative interactions are indicated with a minus. Black boxes indicate interactions that were not tested.

2. GAP activity of Ta-CLO3 and RD20/CLO3

Wheat Ta-CLO3 increases GTP hydrolysis of Ta-GA3

Calcium release is a downstream signaling consequence of Phospholipase C (PLC) activation, and the hydrolysis of GTP is the

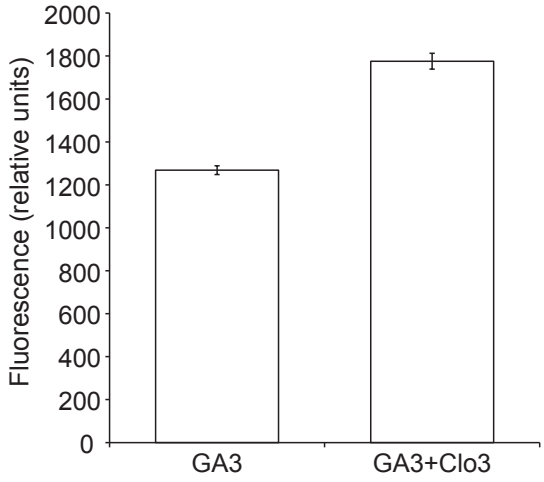

Figure 3. CLO3 stimulation of GA3 GTPase activity. GA3-GST and CLO3-His were expressed in E. coli and purified with affinity matrices for the GST and 6-His-tags, respectively. The proteins were incubated in equimolar amounts with 10 μM GTP in the presence of 10 mM CaCl2 for 30 min. GTPase activity was assayed by measuring Pi released in the reaction mix by a fluorescence emission assay. CLO3 showed no GTPase activity when it was assayed alone. The difference shown is statistically significant.

critical regulatory step in inactivation of G proteins. Consequently, the role of the CLO3 interaction with GA3 was investigated by characterizing the effect of protein–protein interactions on the GTPase activity of Ta-GA3. Ta-GA3-GST and Ta-CLO3-His-fusion proteins were purified from *E. coli* cultures and assayed for GTPase activity in the presence of calcium. Ta-GA3-GST alone showed intrinsic GTPase activity *in vitro* and the activity was stimulated 25% by the equimolar addition of CLO3-His in the presence of calcium as shown in **Fig. 5**. Ta-CLO3 alone showed no GTPase activity. This level of GAP activity was similar to that reported for the Arabidopsis PLDα1 (Zhao and Wang 2004).

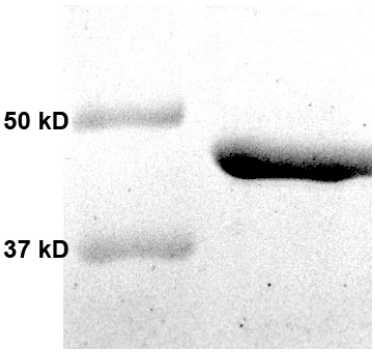

Figure 4. SDS-PAGE showing purified GPA1-His (lane 2), 46.5 kDa in size, shown next to two markers (lane 1).

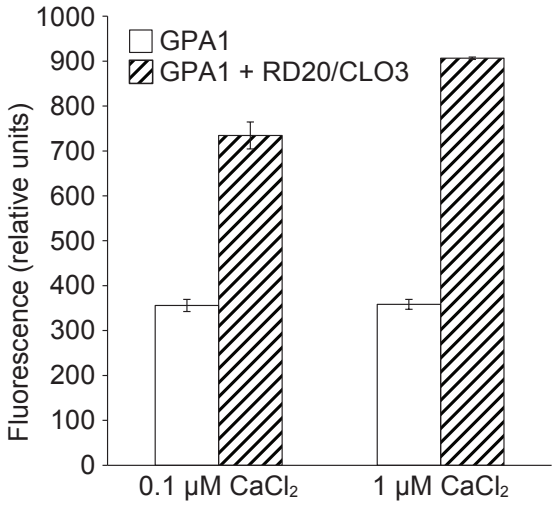

Figure 5. RD20/CLO3 increases the GTPase activity of GPA1. RD20/CLO3-His and GPA1-His were expressed in *E. coli*, purified, and assayed for GTPase activity with 10 μM GTP along with the indicated calcium concentration for 30 min; the GTPase activity was measured by the release of P_i and readings were taken over a period of an hour using a fluorometric assay. Error bars represent standard error. Results are representative of three independent experiments. All samples except the two "GPA1" samples showed significant difference.

Arabidopsis RD20/CLO3 increases GTP hydrolysis of At-GPA1

In vitro assays of GPA1 and RD20/CLO3 purified from *E. coli* showed that RD20/CLO3 increased the GTPase activity of GPA1 to more than two times its initial level (**Figure 5**) and high levels of Ca^{2+} further enhanced this GAP activity. RD20/CLO3 increased the GTPase activity of GPA1 by 106% when the assay was carried out at 100 nM Ca^{2+}, the approximate $[Ca^{2+}]_{cyt}$ in plants under normal conditions; however, at 1 μM Ca^{2+}, a level typical of the increased $[Ca^{2+}]_{cyt}$ under stress conditions, RD20/CLO3 enhanced the GTPase activity of GPA1 by 152% (**Figure 5**). Since G proteins are in their active signalling

state when bound to GTP, GAP proteins are generally negative regulators of G proteins. Our results demonstrate that RD20/CLO3 has GAP activity toward GPA1 and therefore appears to act as a negative regulator of GPA1.

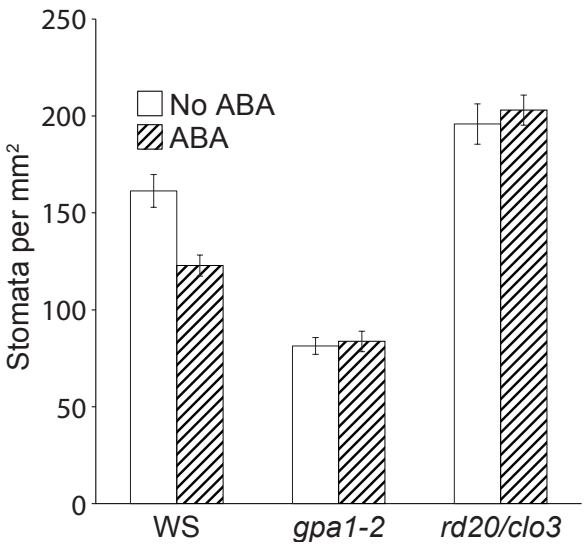

Figure 6. Stomate density in WS, *gpa1-2* and *rd20/clo3* mutant plants, under ABA treatment and control conditions. Six plants were examined in each category and 12 microscope images were taken per plant. Error bars represent standard error. All differences except the two *gpa1-2* samples and the two *rd20/clo3* samples are statistically significant.

3. *RD20/CLO3* mutants have increased stomatal density and altered leaf development

Since *gpa1* mutants in *Arabidopsis* had previously been shown to have increased transpirational efficiency associated with decreased stomatal density (Nilson and Assmann 2010), the effect of the *rd20/clo3* mutation and the effect of ABA treatment on stomatal density was measured (**Figure 6**). Both ABA-treated and untreated 6-week old *rd20/clo3* mutants showed a significant increase in stomatal density, with 203 stomata per mm^2 and 196 stomata per mm^2, respectively. The untreated wild type plants had 161 stomata per mm^2 and ABA treated plants had 123 stomata per mm^2 respectively. In contrast, the untreated *gpa1* mutant had a stomatal density of only 68% of that of wild type, and ABA-treated *gpa1* plants had a stomatal density of only 43% that of ABA treated wild type plants (84 per mm^2 treated, 81 per mm^2 untreated). The decreased stomatal density of *gpa1* mutants measured here is consistent with the results of Nilson and Assmann (2010), and the contrasting effects of the *rd20/clo3* and *gpa1* mutants on stomatal density supports the role of RD20/CLO3 as a negative regulator of GPA1. Both Wassilewskija (WS) and Colombia-0 (Col-0) controls showed a reduction in stomatal density in response to ABA treatment. Since RD20/CLO3 is strongly induced by ABA treatment and environmental stress, and the *rd20/clo3* mutation blocked the effect of ABA treatment on increasing stomatal

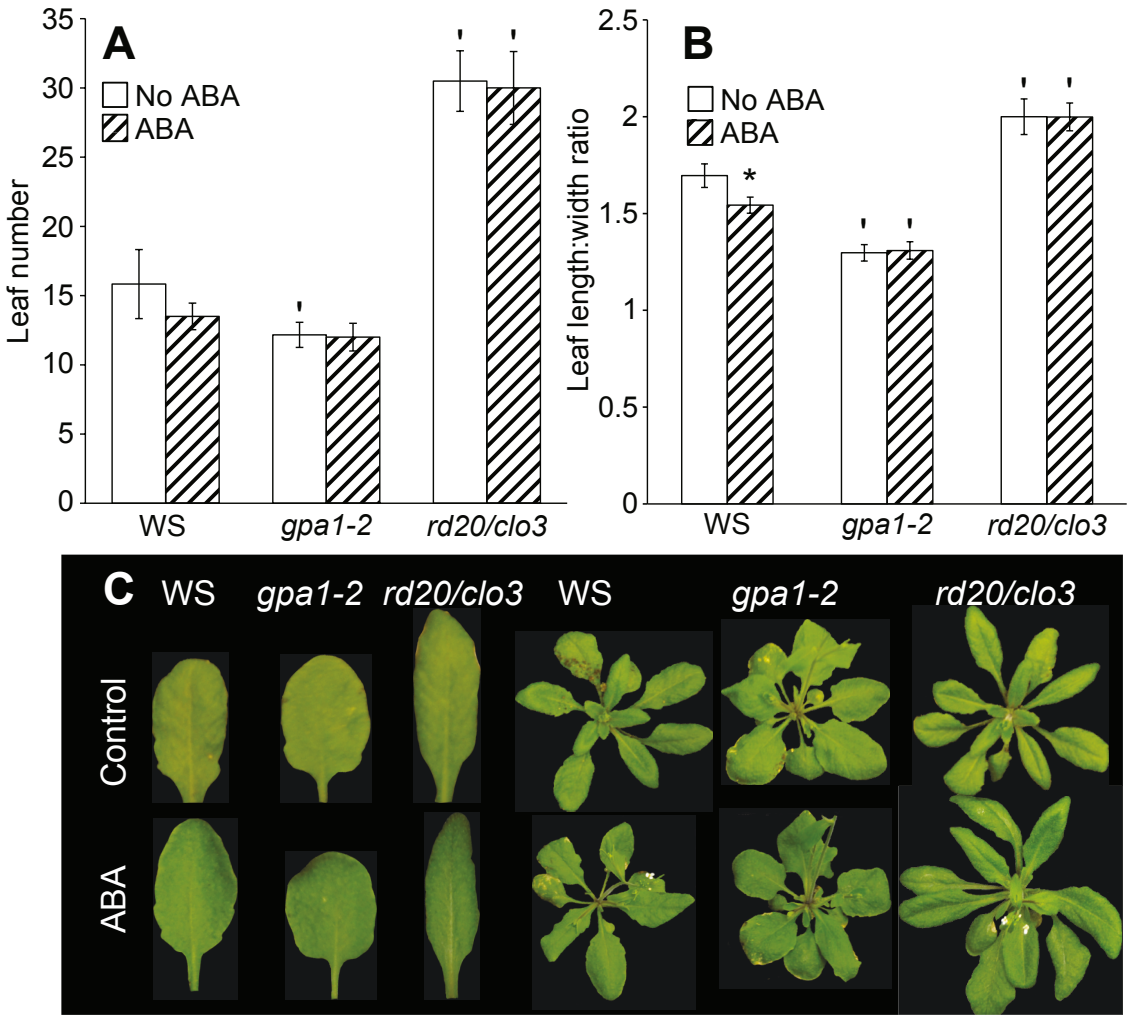

Figure 7. Leaf number and morphology of *rd20/clo3* and *gpa1* mutants. **(A)** Average leaf number of 6 plants (white: untreated, crosshatched: ABA). Error bars represent standard error. **(B)** Average length-to-width ratio in 23-25 leaves as a measure of leaf roundness (white: untreated, crosshatched: ABA). **(C)** Representative images demonstrating leaf morphology of treated and untreated genotypes. * indicates statistical difference between treatment; ' indicates significant difference between genotypes.

density, this gene appears to play an important role in the signalling pathway controlling stomatal differentiation during development and in response to stress. Originally, the experiment design included measurements involving the total number of cells, but limitations in the microscope photography made these measurements impossible.

The effect of the *rd20/clo3* mutation was also seen to have an opposite effect of the *gpa1* mutation on leaf morphology. The leaves of the *rd20/clo3* mutants were significantly narrower than wild type leaves; the mutant had a length:width (l:w) ratio of 2.0 while that of wild type plant leaves was 1.5. Leaves of *gpa1* mutants were the most circular, with an aver-

age l:w ratio of 1.3 (**Figure 7A and B**). ABA treatment also affected the l:w ratio of wild type plants. Leaves on ABA treated WT plants were slightly more round than untreated plants, having a l:w ratio of 1.5, a decrease from the 1.7 of untreated plants. Mutant *rd20/clo3* and *gpa1* did not show an effect of ABA treatment on leaf shape. The *rd20/clo3* mutants showed a large increase in leaf number compared to wild type plants; mutants had average of 30.5 leaves produced before the initiation of flowering, whereas wild type plants had an average of 15.8 leaves (**Figure 7C**). No significant difference was observed in leaf number between ABA-treated and untreated plants.

4. Tissue-specific localization

In order for the previous results to be meaninful, it was important to establish the plausibility of RD20/CLO3 and GPA1 interacting *in vivo,* rather than only *in vitro*. Ex-

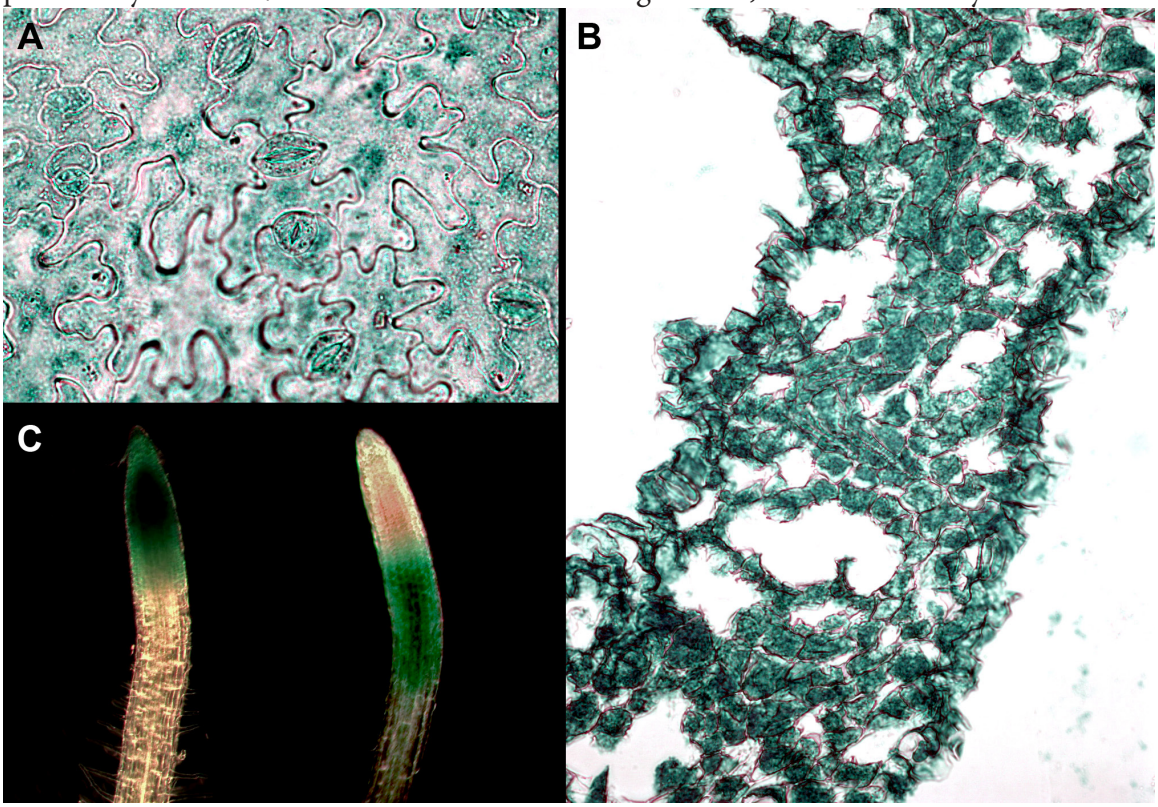

Figure 8. Histochemical GUS staining of transgenic Arabidopsis plants transformed with a *promoterRD20:GUS* reporter construct. **(A) Leaves of** 13-day old plants sprayed twice with 25 μM ABA. **(B)** Plate-grown 10-day old plants were treated with 10 μM ABA for 6h. Leaves were embedded in paraffin, and sectioned to 3 microns thick samples. **(C)** *RD20/CLO3* expression in the root system of the plant after 6h 10 μM ABA treatment. On the left: a 3-day-old primary root; on the right: a 6-day-old lateral root.

periments were therefore performed to verify that there was overlap in the localization of these two proteins. Transgenic plants expressing β-glucuronidase (GUS) under regulation of the *RD20/CLO3* promoter were used to investigate the tissue-specific localization of RD20/CLO3. Previous work (Aubert et al. 2010) examined *RD20/CLO3* expression in Arabidopsis by GUS reporter assay, but failed to detect gene expression in roots, and only examined mature plants. In 13-day-old soil-ground seedlings, epidermal peels showed expression of *RD20/CLO3* throughout the entire leaf, including stomata (**Figure 8A**). This expression appeared both with ABA treatment (sprayed twice per week with 25 μM ABA) and without (sprayed twice per week in control solution with no ABA). This was confirmed by tissue-mounted samples examining 10-day-old plate-grown seedlings treated with ABA for 6 hours (**Figure 8B**). Areas with no expression appeared white when stained.

This study contained a preliminary examination of gene expression in root tissue. A more thorough analysis of *RD20/CLO3* expression in the root was performed by another lab member; these results are described in the discussion. ABA treatment induced *RD20/CLO3* gene expression in roots in a developmentally regulated fashion. In early root development, seedlings with only a primary root showed *RD20/CLO3* induction in the primary root tip. In contrast, six-day-old plants which had both long lateral roots and shorter visibly emerged lateral roots did not show induction of gene expression in the primary root tip or any other part of the primary root; however, these plants showed relatively strong *RD20/CLO3* expression in the lateral roots in the elongation region adjacent to the root tip (**Figure 8C**). Control plants showed no *RD20/CLO3* expression in the root system. The characterization of *promoterGPA1:GUS* transgenic plants showed relatively uniform expression in primary and lateral roots which verifies that the two genes are expressed in the same tissue. The differential expression of *RD20/CLO3* between the primary root and the lateral roots in response to ABA treatment is an intriguing element of the plants' stress response, and suggests that *RD20/CLO3* plays a role in the differentiation between primary and lateral roots in response to environmental stress.

DISCUSSION

1. RD20 is a negative regulator of GPA1 and plays a key role in regulating stomate density in response to ABA treatment

Enzymatic characterization of GPA1 and its interaction with RD20/CLO3 indicate that the stress-induced RD20/CLO3 is a negative regulator of GPA1. The GAP activity exhibited by RD20/CLO3 is expected to down-regulate GPA1 since the active signalling state for G-proteins is the GTP-bound form. The role of *RD20/CLO3* as a negative regulator is confirmed by phenotypic characteristics of the *rd20/clo3* mutant that were the opposite of those of the *gpa1* mutant, as is expected for a negative regulator of GPA1. The *rd20/clo3* mutant had increased stomatal density, whereas the *gpa1* mutant had reduced stomate density. The *rd20/clo3* mutant had more elongated leaves than WT. This was contrary to the case with *gpa1* mutants whose nearly round leaves had a significantly lower length:width ratio than WT (Chen *et al.* 2006). Mutants for *rd20*/clo3 have been shown to be less tolerant to environmental stress (Aubert *et al*. 2010) and the reduced stomatal density is one characteristic reported to be associated with the increased transpirational efficiency observed in the *gpa1* mutant (Nilson and Assman 2010). ABA treatment strongly induces the expression of *RD20/CLO3* (Takahashi *et al*. 2000) and the results reported here demonstrate that it decreases stomate density in WT plants. The observation that ABA treatment did not decrease stomate density in the *rd20/clo3* mutant indicates that *RD20/CLO3* plays a key regulatory role in this response. The evidence for RD20/CLO3's GAP activity with GPA1 and opposite effect of *rd20/clo3* mutant and *gpa1* mutants on stomatal density indicates that the regulation of stomatal density is mediated by *RD20/CLO3* which likely acts as a negative regulator of *GPA1*.

2. Altered expression of RD20/Clo3 results in altered root architecture

The results presented in this study complement the experiments performed by other members of this lab, particularly those of Sabrina Brunetti, who focussed on below-ground tissue. In controlled growth experiments on agar based media, mutants for *rd20/clo3* had less suppression of lateral root emergence and showed a greater reduction in primary root length under ABA treatment than the wild-type control (WS), an effect opposite to that of auxin (Booker *et al.* 2010).

These mutant phenotypes are congruent with the predicted pattern of root development for a negative regulator of GPA1. The results show an increase in lateral root number in *rd20/clo3* mutant plants in response to ABA which is consistent with a role of *RD20/CLO3* as a suppressor of lateral root development and a negative regulator of *GAP1* in the signalling pathways affecting later root development.

3. Plant-wide expression data suggests co-localization between RD20/CLO3 and GPA1

GUS assay results confirm the expression of *RD20/CLO3* in leaf stomatal cells, where *GPA1* is already known to be expressed (Nilson and Assmann 2010). Although Aubert *et al.* (2010) had already found *RD20/CLO3* expression in stomata, only mature plant leaves were examined, while Nilson and Assmann (2010) only found *GPA1* expression in the stomata of young plants. *RD20/CLO3* expression was therefore examined in young plants. This was important for two reasons: first, *RD20/CLO3* was being examined for long-term developmental changes rather than an immediate response, and second, the hypothesis that *RD20/CLO3* is a regulator of *GPA1* predicts that they must be expressed in the same tissue. The analysis of the expression pattern of RD20/CLO3 with a promoter:*GUS* fusion confirmed that *RD20/CLO3* was expressed throughout the leaf in young seedlings, including in the stomatal cells.

A similar analysis was performed to examine root tissue expression, and was later

expanded upon by Sabrina Brunetti. *RD20/CLO3* showed expression in the root tip following ABA treatment, suggesting a role in regulating the emergence and elongation of the primary and lateral roots in response to stress, a notion that is strongly reinforced by experiments examining root architecture. Although Aubert *et al.* (2010) did not observe expression of *RD20/CLO3* in roots, this was likely due to the limited number of environmental conditions under which they tested expression. A very rapid induction of the *RD20/CLO3* promoter:*GUS* reporter by ABA in the elongation zone of lateral roots and the slightly delayed expression throughout most of the root system with the exception of the primary root tip and lower part of the primary root was found. These results are consistent with a role for RD20/CLO3 as an inhibitor of lateral root elongation and lateral root emergence. The characterization of *GPA1* promoter:GUS expression showed expression universally throughout the root tissue, demonstrating that *RD20/CLO3* and *GPA1* are co-expressed in some of the same cell types under stress conditions and are likely to interact *in planta*.

4. Localization and protein-protein interaction suggests that RD20/CLO3 inactivates GPA1 after it is released from the plasma membrane and is likely a downstream regulator

The classical model of heterotrimeric G-protein signalling suggests several steps at which protein-protein interaction may be important for the regulation of Gα; these include the initial trafficking and complex formation at the PM, release from the heterotrimeric complex, interaction with modulating proteins affecting GTPase and GDP/GTP exchange activity, interaction with downstream signalling proteins such as phospholipases C and D, and reconstitution of the G-protein complex at the PM. The ER was reported to be the site for the initial formation of the heterotrimetric complex as well as for Gα palmitoylation before transport to the plasma membrane (Marrari *et al.* 2007). Previous work by Zhejun Wang showed that the GFP-tagged GPA1 was localized to the plasma membrane, while GFP-tagged RD20/CLO3 was localized to the ER. BiFC data showed that the interaction

between the two proteins takes place in or on the ER. This raises the possibility that that the interaction occurs after the release of GPA1 from the plasma membrane, and that RD20/CLO3 down-regulates GPA1 after it has been activated and released from the heterotrimeric complex. To test the alternate hypothesis that RD20/CLO3 sequesters GPA1 in the ER after its synthesis and during its initial transport to the PM, the full length RD20/CLO3:mCherry was co-expressed with a GPA1:eGFP fusion to see if high levels of RD20/CLO3 expression would cause AtGPA1 to be accumulated in the ER rather than the PM, but no evidence was found for this effect.

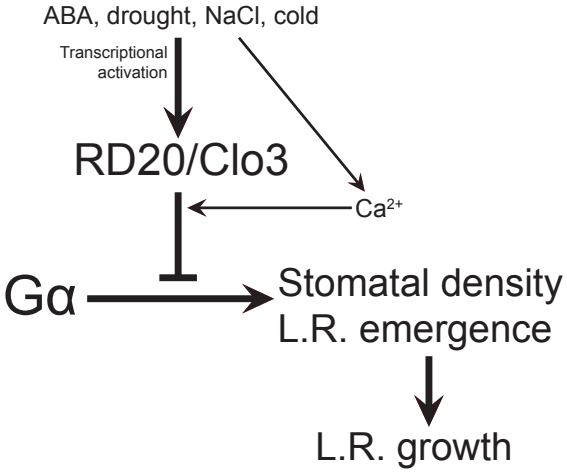

Figure 9. Schematic diagram depicting the *RD20/CLO3* ABA-dependent signaling pathway on lateral root formation and stomata production in Arabidopsis. Based on this study, ABA was shown to induce *RD20/CLO3*, which inhibits Gα's stimulation of lateral root emergence and stomata production.

GAP activity assays of RD20/CLO3 and GPA1, which showed that RD20/CLO3 increases GPA1's rate of GTP hydrolysis, also support the notion that RD20/CLO3 acts as a GPA1 inactivator rather than as an inhibitor of GPA1 transport. In the classic models of heterotrimeric G-protein signalling, the release of Gα from the complex stimulates its activation and is associated with an exchange of GDP for GTP, and its subsequent inactivation is stimulated by its inherent GTPase activity and its association with GAP proteins; the hydrolysis of GTP into GDP precedes its reassociation with Gβγ (Jones *et al.* 2002). The localization of the interaction between GPA1 and RD20/CLO3 away from the PM also suggests that RD20/CLO3 is a downstream inhibitor of GPA1 that interacts with GPA1 after it has been released from the PM. The GAP activity of RD20/CLO3 appears to be significantly more subtle than that of AtRGS1, the only known G-protein coupled receptor in Arabidopsis. The intrinsic GTPase activity of GPA1 was found to be enhanced 15 fold by AtRGS1. It is hypothesized that the GAP activity of the receptor is to retain GPA1 in its membrane-bound inactive

state until stimulated by a ligand (Jones *et al*. 2011). The evidence presented in this study suggests that RD20/CLO3 acts as a transient signal to favour the return of Gα to its inactive GDP-bound state.

Under environmental stress conditions, the cytosolic Ca^{2+} concentration can increase from normal levels of approximately 100 nM into the micromolar range (Lynch *et al.* 1989, Henriksson and Henriksson 2005, Knight *et al.* 1997, Cramer and Jones 1996, D'Onofrio and Lindberg 2009, Kader and Lindberg, 2010). Due to the rise in Ca^{2+} concentration observed under stress, GTPase activity of GPA1 was measured under both low (100 nM) and high (1 μM) concentrations of Ca^{2+}. While the GAP activity of RD20/CLO3 at 1 μM $CaCl_2$ was moderately higher (approximately 25%) than at 100 nM $CaCl_2$, the GTPase activity of GPA1 was increased by over 100% in the presence of RD20/CLO3 at low Ca^{2+} concentrations, suggesting that the effect of RD20/CLO3 on GPA1 is primarily a result of increased *RD20/CLO3* transcription, and to a lesser extent as a result of the Ca^{2+} influx.

The GAP activity reported for RD20/CLO3 is consistent the findings that wheat Ta-*CLO3* acts as a GAP with the wheat Gα, *GA3*. The homology between the Arabidopsis *GPA1* and wheat *GA3* is clear based on their high degree of similarity, 87% amino acid sequence similarity, as well as the fact that Gα is a single gene in Arabidopsis and that there are three known Gα's in wheat. However, the caleosins are represented by a six member gene family in Arabidopsis and 11 genes in the diploid genome of wheat. *RD20/CLO3* is one of Arabidopsis caleosin genes most similar to Ta-*CLO3* but their 63% amino acid sequence identity by itself is not sufficient to establish orthology between the two genes. The fact that they have been shown to associate with Gα both *in vivo* and i*n vitro* and that they have GAP activity suggests that they play similar roles in the two species. The characterization of mutants, and promoter:*GUS* lines in Arabidopsis provides an insight into the role of one member of the caleosin gene family that would be difficult to achieve in cereals at this time. This work underscores the value of model species in the characterization of stress regulated genes discovered through genomic analysis, and encourages the development of

genetic tools for monocot model species such as *Brachypodium*. The characterization of other members of the caleosin gene family has yet to be carried out, and their potential role in signalling and regulation remains to be investigated.

5. BiFC results revealed novel interactions between G-proteins and caleosins

The three caleosins examined in this study were chosen to encompass varying degrees of diversity in the caleosin gene family. *RD20/CLO3* is the closest homolog to Ta-*CLO3* in wheat by amino acid sequence, while At-*CLO7* is the furthest. At-*CLO2* is one of the closest genes in the Arabidopsis caleosin family to *RD20/CLO3*. A comparison of common sequences and the interactors associated with them will help reveal the active regions in these proteins. Given the relationship between these three genes, it is surprising that RD20/CLO3 and CLO7 both interact with GPA1, while CLO2 was not found to interact with any G-protein. Because there are no known interactors of CLO2, it could not be determined whether the lack of interactions with CLO2 were genuine, or simply a problem with the chimeric protein.

Both CLO7-v1 and Gγ, when expressed as a fusion with eGFP, were both localized to the nucleus and what appears to be the plasma membrane, while the interaction between the two proteins did not take place in the nucleus at all.

6. RD20/Clo3's inhibition of GPA1 is consistent with standard plant physiological stress response

The opposite phenotypes exhibited by *rd20/clo3* and *gpa1* mutants are not only predicted by the hypothesis of *RD20/CLO3* as a downregulator of *GPA1*; they are also consistent with the expected physiological stress response. The drastic increase in stomatal density seen in *rd20/clo3* mutants suggests that the increased expression of *RD20/CLO3* in response

to drought allows the leaves to develop with fewer stomata, thereby decreasing water loss. The decrease in stomatal density observed in *gpa1* mutants suggests that this result can be achieved by the downregulation of *GPA1.* Similarly, in roots, the decrease in primary root length and increase in lateral root number in *rd20/clo3* mutants suggests that the increased expression of *RD20/CLO3* in response to drought allows the root to penetrate deeper into the soil to find water, a recognized drought adaptation in Arabidopsis (Xiong *et al.* 2006).

Research by Chen *et al.* (2006) suggests that many of the phenotypes shown by *GPA1* can be attributed to its stimulation of cell division. These phenotypes of *gpa1* mutants included the decrease in stomatal density and changes in leaf morphology. This effect may account for the changes in stomatal density in *rd20/clo3* mutants. The effect is also consistent with the altered lateral root production, which mostly occurred in the form of changes in the elongation of lateral root primordia. However, changes in cell division rate do not fully account for this phenotype, because in unpublished data from other lab members, *rd20/clo3* mutants also showed a slight increase in lateral root primordia, suggesting that *RD20/CLO3* has a minor effect on cell differentiation in addition to its suppression of cell division.

7. Conclusion

This study intended to characterize the interaction between *RD20/CLO3* and *GPA1,* and to determine the role of this interaction in plant stress response. The GAP activity exhibited by RD20/CLO3 toward GPA1, seen both with the Arabidopsis genes as well as their closest homologs in wheat, suggests that RD20/CLO3 acts by inactivating GPA1 in response to ABA and calcium. Phenotypic analysis of *rd20/clo3* and *gpa1* mutants consistently showed a pattern of opposite phenotypes congruent with the hypothesis of downregulation. GUS analysis confirms that the interaction may take place *in planta.* Because very few GAPs have been found in plant G-protein complexes, the discovery of *RD20/CLO3* as

a novel GAP provides an important contribution to our understanding of plant G-protein signalling as well as insight into the role of the caleosin gene family.

REFERENCES

Aharon G.S., Gelli, A., Snedden, W.A., and Blumwald, E. (1998). Activation of a plant plasma membrane Ca2+ channel by TGalpha1, a heterotrimeric G protein alpha-subunit homologue. FEBS Lett. **424:** 17-21.

Allen, G.J., Chu, S.P., Harrington, C.L., Schumacher, K., Hoffmann, T., Tang, Y.Y., Grill, E., and Schroeder, J.I. (2001). A defined range of guard cell calcium oscillation parameters encodes stomatal movements. Nature **411:** 1053-1057.

Aubert, Y., Vile, D., Pervent, M., Aldon, D., Ranty, B., Simonneau, T., Vavasseur, A., and Galaud, J.P. (2010). RD20, a stress-inducible caleosin, participates in stomatal control, transpiration and drought tolerance in Arabidopsis thaliana. Plant Cell Physiol. **51:** 1975-1987.

Bent, A. (2006) *Arabidopsis thaliana* floral dip transformation method. Methods Mol. Biol. **343:** 87-103.

Booker, K.S., Schwarz, J., Garrett, M.B., and Jones, A.M. (2010). Glucose Attenuation of Auxin-Mediated Bimodality in Lateral Root Formation Is Partly Coupled by the Heterotrimeric G Protein Complex. PMID: 20862254.

Cattivelli, L., Rizza, F., Badeck, F.W., Mazzucotelli, E., Mastrangelo, A.M., Francia, E., Marè, C., Tondelli, A., and Stanca, A.M. (2008). Drought tolerance improvement in crop plants: An integrated view from breeding to genomics, Field Crops Research **105:** 1-14.

Chen, H., and Jiang, J.-G. (2010). Osmotic adjustment and plant adaptation to environmental changes related to drought and salinity. Environmental Reviews **18:** 309-319.

Chen, J.G., Gao, Y., and Jones, A.M. (2006). Differential roles of Arabidopsis heterotrimeric G-protein subunits in modulating cell division in roots. Plant Physiol. **141:** 87-897.

Chen, J.G., Willard, F.S., Huang, J., Liang, J., Chasse, S.A., Jones, A.M., and Siderovski, D.P. (2003). A seven-transmembrane RGS protein that modulates plant cell proliferation. Science **301:** 1728-1731.

Clough, S.J., and Bent, A.F. (1998). Floral dip: a simplified method for *Agrobacterium-*

mediated transformation of *Arabidopsis thaliana.* Plant J. **16:** 736-743.

Cramer, G., and Jones, R. (1996). Osmotic stress and abscisic acid reduce cytosolic calcium activities in roots of Arabidopsis thaliana*. Plant, Cell & Environment **19:** 1291-1298.

D'Onofrio, C., and Lindberg, S. (2009). Sodium induces simultaneous changes in cytosolic calcium and pH in salt-tolerant quince protoplasts. Journal of plant physiology **166:** 1755-1763.

Dodd, A.N., Kudla, J., and Sanders, D. (2010). The language of calcium signaling. Annual review of plant biology **61:** 593-620.

Dubrovsky, J.G., and Forde, B.G. (2012). Quantitative Analysis of Lateral Root Development: Pitfalls and How to Avoid Them. Plant Cell **24:** 4-14.

Fleury, D., Jefferies, S., Kuchel, H., and Langridge, P. (2010). Genetic and genomic tools to improve drought tolerance in wheat. Journal of Experimental Botany **61:** 3211-3222.

Grigston, J.C., Osuna, D., Scheible, W.R., Liu, C., Stitt, M., and Jones, A.M. (2008). D-Glucose sensing by a plasma membrane regulator of G signaling protein, AtRGS1. FEBS Lett. **582:** 3577–3584

Gulick, P.J., Drouin, S., Yu, Z., and Danyluk, J. (2005). Transcriptome comparison of winter and spring wheat responding to low temperature. Genome **48:** 913-923.

Heinze, M., Steighardt, J., Gesell, A., Schwartze, W., and Roos, W. (2007). Regulatory interaction of the Gα protein with phospholipase A_2 in the plasma membrane of *Eschscholzia californica.* Plant J. **52:** 1041-1051.

Henriksson, E., and Nordin Henriksson, K. (2005). Salt-stress signalling and the role of calcium in the regulation of the Arabidopsis ATHB7 gene. Plant, Cell & Environment **28:** 202-210.

Holtz, U. (2007). Implementing the United Nations Convention to Combat Desertification from a parliamentary point of view - Critical assessment and challenges ahead. http://www.unccd.int/Lists/SiteDocumentLibrary/Parliament/2007/parliamentariansforum.pdf

Huang, J.R., Taylor, J.P., Chen, J.C., Uhrig, J.F., Schnell, D.J., Nakagawa, T., Korth, K.L., and Jones, A.M. (2006). The plastid protein THYLAKOID FORMATION1 and the plasma membrane G-protein GPA1 interact in a novel sugar-signaling mechanism

in Arabidopsis. Plant Cell **18:** 1226-1238.

Jefferson, R.A., Kavanagh, T.A., and Bevan, M.W. (1987). GUS fusions: beta-glucoronidase as a sensitive and versatile gene fusion marker in higher plants. EMBO J. **6:** 3901-3907.

Jones, A.M. (2002). G-protein-coupled signaling in *Arabidopsis*. Curr. Opin. Plant Biol. **5**: 402–407.

Jones, A.M., and Assmann, S.M. (2004). Plants: the latest model system for G-protein research. EMBO Rep. **5:** 572-578.

Jones, J.C., Temple, B.R.S., Jones, A.M., and Dohlman, H.G. (2011). Functional Reconstitution of an Atypical G Protein Heterotrimer and Regulator of G Protein Signaling Protein (RGS1) from Arabidopsis thaliana. Journal of Biological Chemistry **286:** 13143-13150.

Kader, M.A., and Lindberg, S. (2010). Cytosolic calcium and pH signaling in plants under salinity stress. Plant signaling & behavior **5:** 233-238.

Kapila, J., De Rycke, R., and Angenon, G. (1997). An Agrobacterium-mediated transient gene expression system for intact leaves. Plant Sci. **122:** 101–108.

Khalil, H.B., Wang, Z., Wright, J.A., Ralevski, A., Donayo, A.O., and Gulick, P.J. (2011). Heterotrimeric Gα subunit from wheat (Triticum aestivum), GA3, interacts with the calcium-binding protein, Clo3, and the phosphoinositide-specific phospholipase C, PI-PLC1. Plant Mol. Biol. **77:** 145-158.

Kim, Y.Y., Jung, K.W., Yoo, K.S., Jeung, J.U., and Shin, J.S. (2011). A stress-responsive caleosin-like protein, AtCLO4, acts as a negative regulator of ABA responses in Arabidopsis. Plant & cell physiology **52:** 874-884.

Knight, H., Trewavas, A.J., and Knight, M.R. (1997). Calcium signalling in Arabidopsis thaliana responding to drought and salinity. The Plant Journal **12:** 1067-1078.

Kreps, J.A., Wu, Y., Chang, H.-S., Zhu, T., Wang, X., and Harper, J.F. (2002) Transcriptome changes for Arabidopsis in response to salt, osmotic and cold stress. Plant Physiol. **130:** 2129–2141.

Lapik, Y.R., and Kaufman, L.S. (2003). The Arabidopsis cupin domain protein AtPirin 1 interacts with the G protein α-subunit GPA1 and regulates seed germination and early seedling development. Plant Cell **15:** 1578-1590.

Lecourieux, D., Lamotte, O., Bourque, S., Wendehenne, D., Mazars, C., Ranjeva, R., and Pugin, A. (2005). Proteinaceous and oligosaccharidic elicitors induce different calcium signatures in the nucleus of tobacco cells. Cell Calcium **38:** 527-538.

Luan, S. (2009). The CBL-CIPK network in plant calcium signaling. Trends in plant science **14:** 37-42.

Lynch, J., Polito, V.S., and Läuchli, A. (1989). Salinity stress increases cytoplasmic Ca activity in maize root protoplasts. Plant physiology **90:** 1271-1274.

Malamy, J.E., and Benfey, P.N. (1997). Organization and cell differentiation in lateral roots of *Arabidopsis thaliana*. Development **124:** 33-44.

Marrari, Y., Crouthamel, M., Irannejad, R., and Wedegaertner, P.B. (2007). Assembly and trafficking of heterotrimeric G proteins. Biochemistry **46:** 7665-7677.

Misra, S., Wu, Y., Venkataraman, G., Sopory, S.K., and Tuteja, N. (2007). Heterotrimeric G-protein complex and G-protein-coupled receptor from a legume (Pisum sativum): role in salinity and heat stress and cross-talk with phospholipase C. Plant J. **51:** 656–669.

Monroy, A.F., Dryanova, A., Malette, B., Oren, D.H., Ridha Farajalla, M., Liu, W., Danyluk, J., Ubayasena, L.W.C., Kane, K., Scole, G.S., Sarhan, F., and Gulick, P.J. (2007). Regulatory gene candidates and gene expression analysis of cold acclimation in winter and spring wheat. Plant Mol. Biol. **64:** 409-423.

Mori, I.C., Murata, Y., Yang, Y., Munemasa, S., Wang, Y.-F., Andreoli, S., Tiriac, H., Alonso, J.M., Harper, J.F., Ecker, J.R., *et al.* (2006). CDPKs CPK6 and CPK3 Function in ABA Regulation of Guard Cell S-Type Anion- and Ca²⁺- Permeable Channels and Stomatal Closure. PLoS Biol **4:** e327.

Naested, H., Frandsen, G.I., Jauh, G.Y., Hernandez-Pinzon, I., Nielsen, H.B., Murphy, D.J., Rogers, J.C., and Mundy, J. (2000). Caleosins: Ca2+-binding proteins associated with lipid bodies. Plant molecular biology **44:** 463-476.

Nilson, S.E., and Assmann, S.M. (2010). The alpha-subunit of the Arabidopsis heterotrimeric G protein, GPA1 is a regulator of transpiration efficiency. Plant Physiol. **152:** 2067-2077.

Okamoto, M., Tanaka, Y., Abrams, S.R., Kamiya, Y., Seki, M., and Nambara, E. (2009) High Humidity Induces Abscisic Acid 8cHigh Humidity Induces Abscisic Kamiya, Y., Seki, M., and Nambara, E.gulAbscisic Acid Responses in Arabidopsis. Plant

Physiol. **149:** 825-834.

Oono, Y., Seki, M., Nanjo, T., Narusaka, M., Fujita, M., Satoh, R., Satou, M., Sakurai, T., Ishida, J., Akiyama, K., Lida, K., Maruyama, K., Satoh, S., Yamaguchi-Shinozaki, K., and Shhinozaki, K. (2003). Monitoring expression profiles of *Arabidopsis* gene expression during rehydration process after dehydration using *ca.* 7000 full-length cDNA microarray. Plant J. **34:** 868–887.

Pandey, S., and Assmann, S.M. (2004). The Arabidopsis putative G protein-coupled receptor GCR1 interacts with the G protein alpha subunit GPA1 and regulates abscisic acid signaling. Plant Cell **16:** 1616-1632.

Pandey, S., Chen, J.G., Jones, A.M., and Assmann, S.M. (2006). G-protein complex mutants are hypersensitive to abscisic acid regulation of germination and postgermination development. Plant Physiol. **141:** 243-56.

Pandey, S., Nelson, D.C., and Assmann, S.M. (2009). Two novel GPCR-type G proteins are abscisic acid receptors in Arabidopsis. Cell **136:** 136-148.

Ritchie, S., and Gilroy, S. (2000). Abscisic acid stimulation of phospholipase D in the barley aleurone is G-protein-mediated and localized to the plasma membrane. Plant Physiol. **124:** 693–702.

Sanders, D., Pelloux, J., Brownlee, C., and Harper, J.F. (2002). Calcium at the Crossroads of Signaling. The Plant Cell Online **14:** S401-S417.

Steffens, B., and Sauter, S. (2010). G proteins as regulators in ethylene-mediated hypoxia signalling. Plant Signal. Behav. **5:** 375–378.

Takahashi, S., Katagiri, T., Yamaguchi-Shinozaki, K., and Shinozaki, K. (2000). An arabidopsis gene encoding a Ca 2+ -binding protein is induced by abscisic acid during dehydration. Plant Cell Physiol. **41:** 898-903.

Tardif, G., Kane, N.A., Adam, H., Labrie, L., Major, G., Gulick, P., Sarhan, F., and Laliberte, J.F. (2007). Interaction network of proteins associated with abiotic stress response and development in wheat. Plant Mol. Biol. **63:** 703-718.

Ullah, H., Chen, J.G., Temple, B., Alonso, J., Ecker, J., Boyes, D., Davis, K., and Jones, A.M. (2003). Plant Cell **15:** 393-409.

Urano, D., and Jones, A.M. (2013). "Round Up the Usual Suspects": A Comment on Nonexistent Plant G Protein-Coupled Receptors. Plant physiology **161:** 1097-1102.

Wang, X., Ullah, H., Jones, A.J., and Assmann, S.M. (2001). G Protein Regulation of Ion Channels and Abscisic Acid Signaling in Arabidopsis Guard Cells. Science **292:** 2070-2072.

Warpeha, K.M., Lateef, S.S., Lapik, Y., Anderson, M., Lee, B.S., and Kaufman, L.S. (2006). G-protein-coupled receptor 1, G-protein Galpha-subunit 1, and prephenate dehydratase 1 are required for blue light-induced production of phenylalanine in etiolated Arabidopsis. Plant Physiol. **140:** 844-855.

Willard, F.S., and Siderovski, D.P. (2004). Purification and in vitro functional analysis of the Arabidopsis thaliana Regulator of G-Protein Signaling-1. Methods Enzymol. **389:** 320-337.

World Bank, Food and Agriculture Organization of the United Nations, International Fund for Agricultural Development. (2009). Gender in Agriculture Sourcebook. (World Bank Publications) pp. 454-455.

Wurzinger, B., Mair, A., Pfister, B., and Teige, M. (2011). Cross-talk of calcium-dependent protein kinase and MAP kinase signaling. Plant Signaling & Behavior **6:** 8-12.

Xing, M., Du, Y., Wang, X., Niu, L., and Chen, X. (2010). A simplified paraffin embedding method for small botanical samples. Biotechnic & histochemistry : official publication of the Biological Stain Commission **85:** 241-246.

Xiong, L.M., Wang, R.G., Mao, G.H., and Koczan, J.M. (2006). Identification of drought tolerance determinants by genetic analysis of root response to drought stress and abscisic acid. Plant Physiol. **142:** 1065–1074.

Yaish, M.W., Colasanti, J., and Rothstein, S.J. (2011). The role of epigenetic processes in controlling flowering time in plants exposed to stress. Journal of Experimental Botany.

Zhao, J., and Wang, X. (2004). Arabidopsis phospholipase Dalpha1 interacts with the heterotrimeric G-protein alpha-subunit through a motif analogous to the DRY motif in G-protein-coupled receptors. J. Biol. Chem. **279:** 1794-1800.

Zolla, G., Heimer, Y.M., and Barak, S. (2010). Mild salinity stimulates a stress-induced morphogenic response in Arabidopsis thaliana roots. J Exp Bot. **61**:211-24.